Original Article

Opportunistic use of chest low-dose computed tomography (LDCT) imaging for low bone mineral density and osteoporosis screening: cutoff thresholds for the attenuation values of the lower thoracic and upper lumbar vertebrae

Ya-Ling Pan[1#^], Yin-Bo Wu[1#], Huo-Gen Wang[2,3], Tai-Hen Yu[1], Dong He[1], Xiang-Jun Lu[1], Fan-Fan Zhao[1], Hong-Feng Ma[1], Ya-Jie Wang[1], Yun-Kai Cai[4^]

[1]Center for Rehabilitation Medicine, Department of Radiology, Zhejiang Provincial People's Hospital (Affiliated People's Hospital), Hangzhou Medical College, Hangzhou, China; [2]Hithink RoyalFlush Information Network Co., Ltd., Hangzhou, China; [3]Zhejiang Herymed Technology Co., Ltd., Hangzhou, China; [4]Cancer Center, Department of Nuclear Medicine, Zhejiang Provincial People's Hospital (Affiliated People's Hospital), Hangzhou Medical College, Hangzhou, China

Contributions: (I) Conception and design: YL Pan, YK Cai; (II) Administrative support: YL Pan, YJ Wang, YK Cai; (III) Provision of study materials or patients: YL Pan, YB Wu, YJ Wang; (IV) Collection and assembly of data: TH Yu, D He, XJ Lu, FF Zhao, HF Ma, YK Cai; (V) Data analysis and interpretation: YL Pan, YB Wu, HG Wang, YJ Wang, YK Cai; (VI) Manuscript writing: All authors; (VII) Final approval of manuscript: All authors.

[#]These authors contributed equally to this work.

Correspondence to: Yun-Kai Cai, MD. Cancer Center, Department of Nuclear Medicine, Zhejiang Provincial People's Hospital (Affiliated People's Hospital), Hangzhou Medical College, 158 Shangtang Road, Hangzhou 310014, China. Email: caiyunkai94@163.com; Ya-Jie Wang, MD. Center for Rehabilitation Medicine, Department of Radiology, Zhejiang Provincial People's Hospital (Affiliated People's Hospital), Hangzhou Medical College, 158 Shangtang Road, Hangzhou 310014, China. Email: wangyajie3964@163.com.

Background: Osteoporosis remains substantially underdiagnosed and undertreated worldwide. Chest low-dose computed tomography (LDCT) may provide a valuable and popular opportunity for osteoporosis screening. This study sought to evaluate the feasibility of the screening of low bone mineral density (BMD) and osteoporosis with mean attenuation values of the lower thoracic compared to upper lumbar vertebrae. The cutoff thresholds of the mean attenuation values in Hounsfield units (HU) were derived to facilitate implementation of opportunistic screening using chest LDCT.

Methods: The participants aged 30 years or older who underwent chest LDCT and quantitative computed tomography (QCT) examinations from August 2018 to October 2020 in our hospital were consecutively included in this retrospective study. A region of interest (ROI) was placed in the trabecular bone of each vertebral body to measure the HU values. The correlations of mean HU values of lower thoracic (T11–T12) and upper lumbar (L1–L2) vertebrae with age and lumbar BMD obtained with QCT were performed using the Pearson correlation coefficient, respectively. The area under the curve (AUC) of the receiver operator characteristic (ROC) curve was generated to determine the cutoff thresholds for distinguishing low BMD from normal and osteoporosis from non-osteoporosis.

Results: A total of 1,112 participants were included in the final study cohort (743 men and 369 women, mean age 58.2±8.9 years; range, 32–88 years). The mean HU values of T11–T12 and L1–L2 were significantly different among 3 QCT-defined BMD categories of osteoporosis, osteopenia, and normal ($P<0.001$). The differences in HU values between T11–T12 and L1–L2 in each category of bone status

^ ORCID: Ya-Ling Pan, 0000-0002-4143-2139; Yun-Kai Cai, 0009-0007-2833-8264.

were statistically significant (P<0.001). The mean HU values of T11–T12 (r=–0.453, P<0.001) and L1–L2 (r=–0.498, P<0.001) had negative correlations with age. Positive correlations were observed between the mean HU values of T11–T12 (r=0.872, P<0.001) and L1–L2 (r=0.899, P<0.001) with BMD. The optimal cutoff thresholds for distinguishing low BMD from normal were average T11–T12 ≤157 HU [AUC =0.941, 95% confidence interval (CI): 0.925–0.954, P<0.001] and L1–L2 ≤138 HU (AUC =0.950, 95% CI: 0.935–0.962, P<0.001), as well as distinguishing osteoporosis from non-osteoporosis were average T11–T12 ≤125 HU (AUC =0.960, 95% CI: 0.947–0.971, P<0.001) and L1–L2 ≤107 HU (AUC =0.961, 95% CI: 0.948–0.972, P<0.001). There was no significant difference between the AUC values of T11–T12 and L1–L2 for low BMD (P=0.07) and osteoporosis (P=0.92) screening.

Conclusions: We have conducted a study on low BMD and osteoporosis screening using mean attenuation values of lower thoracic and upper lumbar vertebrae. Assessment of mean attenuation values of T11–T12 and L1–L2 can be used interchangeably for low BMD and osteoporosis screening using chest LDCT, and their cutoff thresholds were established.

Keywords: Low-dose computed tomography (LDCT); osteoporosis; screening; thoracic vertebrae; trabecular attenuation

Submitted Jan 10, 2024. Accepted for publication May 22, 2024. Published online Jun 24, 2024.
doi: 10.21037/qims-24-59
View this article at: https://dx.doi.org/10.21037/qims-24-59

Introduction

Osteoporosis is a systemic skeletal disease characterized by loss of bone strength and susceptibility to fractures (1). Osteoporotic fractures of the hip and spine are associated with high mortality and morbidity, representing a high economic burden for society (2). Osteoporosis has been defined as a silent epidemic becoming a public health risk due to its severity, chronicity, progression, and that it affects mainly senile people (3). The prevalence of osteoporosis is projected to rapidly increase worldwide with the aging population. Hence, the early screening of osteoporosis plays a significant role in the progress and prevention of this disease.

At present, dual X-ray absorptiometry (DXA) is the most widely used detection tool for osteoporosis (4). However, fewer women and men have received DXA scans than projected since 2008 because of significantly reduced reimbursement for DXA scans in the United States, which resulted in an increase of undiagnosed and untreated osteoporosis of 43% in 2017 (5). As a recognized approach for volumetric bone mineral density (BMD) measurement specifically of trabecular bone, quantitative computed tomography (QCT) holds higher sensitivity and accuracy on osteoporosis diagnosis than DXA (6). However, the application of QCT remains limited by the standardized software, extra calibration, and higher radiation dose (6). Despite the known morbidity associated with osteoporotic fractures and the availability of these diagnostic approaches, osteoporosis remains substantially underdiagnosed and undertreated (7).

The opportunistic use of computed tomography (CT) as a radiological method to assess the risk for low BMD may contribute to increasing screening rates. Several studies (8-10) have entailed measurement of CT attenuation values in Hounsfield units (HU) on the spine from CT imaging, with ensuing statistical correlation with BMD from DXA. The widespread employment of chest low-dose CT (LDCT) imaging in the course of general health examination population provides a particular opportunity for osteoporosis screening at no additional time, cost, or radiation exposure to patients (11). Compared to abdomen-pelvis contrast enhanced CT and lumbar spine CT, chest LDCT has been shown to have the highest diagnostic performance for osteoporosis with predetermined HU cutoff values (12). Some critics have cited scanner-to-scanner variability in HU measurement as the major obstacle (8). Despite that it is not very sufficiently accurate for disease identification, HU measurement in opportunistic screening and preliminary detection of low BMD and osteoporosis for alerting physicians to make a further definite diagnosis has been suggested in many studies (9,10,13).

In most previous studies (12,14,15), trabecular attenuation was usually measured at the L1 level in chest CT and its performance evaluation commonly used DXA as reference standard. A CT-based reference standard of L1 trabecular attenuation for opportunistic osteoporosis screening was constructed in a largely White population (14). Osteoporosis is a diffuse disease that is usually determined with 2 or more vertebrae (e.g., QCT BMD measurement at L1 and L2 level in chest LDCT) (16,17). The number of vertebrae captured in chest CT depends on the field of view, which varies between patients (18). Some hospitals tend to narrow the scan range to reduce radiation exposure, resulting in some chest CT scans not including L1 on unenhanced image (15). To our knowledge, few studies have assessed HU measurement at lower thoracic vertebrae levels in opportunistic osteoporosis screening of a Chinese population. When the L1 and L2 vertebrae were unsuitable for measurement (e.g., vertebral compression fractures or focal abnormality) and not included in chest CT examinations, adjacent T11 and T12 vertebrae serving as acceptable substitutes in practice were expected to be explored.

In this study, we performed opportunistic screening on a Chinese population using chest LDCT to evaluate the feasibility of low BMD and osteoporosis screening with mean attenuation values of the lower thoracic compared to upper lumbar vertebrae, utilizing QCT as reference standard. We aimed to determine the optimal cutoff thresholds for the attenuation values of the lower thoracic and upper lumbar vertebrae in HU to distinguish low BMD from normal and osteoporosis from non-osteoporosis as well as the diagnostic value, which would aid to identify patients at risk who could potentially benefit from further assessment and intervention. We present this article in accordance with the STARD reporting checklist (available at https://qims.amegroups.com/article/view/10.21037/qims-24-59/rc).

Methods

The study was conducted in accordance with the Declaration of Helsinki (as revised in 2013). The study was approved by the Ethics Committee at Zhejiang Provincial People's Hospital (IRB No. 2021QT236) and the requirement for individual consent for this retrospective analysis was waived.

Population cohort

Between August 2018 and October 2020, 1,278 participants aged 30 years or older who underwent chest LDCT and QCT examinations for health check-up in our hospital were consecutively included. We excluded 166 participants with attenuation heterogeneity in the vertebral bodies of T11 to L2, such as bone islands, calcification, tumor, infectious or cystic lesions, surgery, fractures, imaging artifacts, and metabolic bone diseases such as hyperparathyroidism and renal osteodystrophy (*Figure 1*). A total of 1,112 participants were included in the final study cohort (743 men and 369 women, mean age 58.2±8.9 years; range, 32–88 years).

Chest LDCT examination

Chest LDCT scans were performed using 2 CT scanners from different vendor (Somatom Definition AS+, Siemens Healthcare, Erlangen, Germany; Optima CT540, GE Healthcare, Chicago, IL, USA). The following CT protocol in accordance with the "China Health Quantitative CT Big Data Project Research Program" (16) was used: 120 kVp, automated tube current, average 30 mAs, 1.0-mm or 1.25-mm reconstruction slice thickness, 512×512 matrices, and 500-mm scan field of view. To ensure accuracy of CT attenuation numbers, 2 scanners were calibrated daily.

BMD measurement with QCT

An asynchronously phantom (Mindways, Austin, TX, USA) was scanned to calibrate the BMD of lumbar spine with the same chest LDCT parameters. After scanning, the chest LDCT images were transferred to the QCT workstation (Mindways QCT Pro 6.1, Austin, TX, USA) for further analysis. BMD was measured within the cylindrical regions of interest (ROIs), which were 9 mm high and placed in the center of L1 to L2 vertebral bodies avoiding cortical bone and basivertebral veins. The BMD values (mg/cm^3) of L1 and L2 were recorded and analyzed, respectively, and the average was calculated. Each participant bone status was categorized into normal (BMD >120 mg/cm^3), osteopenia (80 mg/cm^3≤ BMD ≤120 mg/cm^3), and osteoporosis (BMD <80 mg/cm^3) in accordance with the American College of Radiology QCT diagnostic criteria (17). Low BMD was defined as BMD ≤120 mg/cm^3, including osteopenia and osteoporosis.

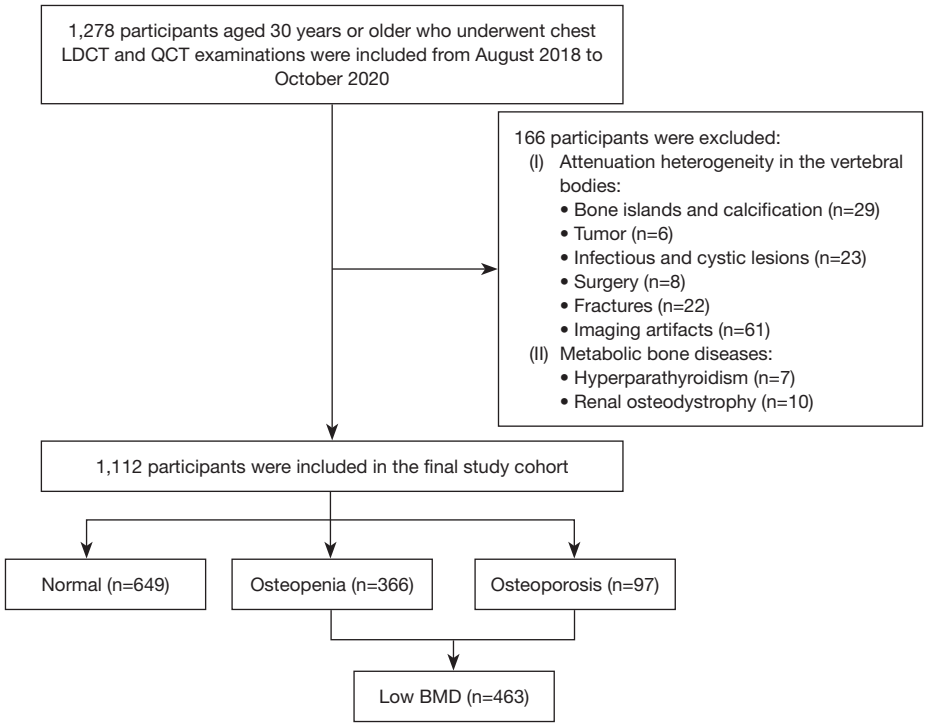

Figure 1 Flowchart of participants inclusion and grouping according to bone status. LDCT, low-dose computed tomography; QCT, quantitative computed tomography; BMD, bone mineral density.

CT attenuation measurement

First, 4 vertebral bodies (T11 to L2) were manually annotated using the ITK-SNAP software (version 3.8; http://itksnap.org). Second, the 3-dimensional (3D) ROI of attenuation measurement was generated from the manual annotation through adaptive morphologic erosion and geometric operations, and located in the center of trabecular bone of vertebral body avoiding cortical bone and basivertebral veins. Our ROIs (height of cylinders =9 mm) for T11 to L2 were similar to the ROIs in QCT BMD measurement (Figure S1). Finally, CT attenuation values within ROIs were automatically calculated and expressed in HU. HU values of individual T11 to L2, and mean HU values of each vertebral combination T11 and T12 (T11–T12) as well as L1 and L2 (L1–L2) were recorded.

Statistical analysis

Statistical analyses were performed using SPSS 22.0 and MedCalc ®v18.11.3. Continuous variables were visually assessed for normal distribution using QQ-plots and expressed as mean ± standard deviation (SD) and 95% confidence interval (CI). One-way analysis of variance (ANOVA) was used to compare the HU values among vertebrae of T11 to L2. Due to heteroscedasticity, Kruskal-Wallis tests were used to compare HU values of T11 to L2 and mean HU values of T11–T12 and L1–L2 of all participants according to QCT categories. We used independent-samples *t*-tests to compare age and HU values between females and males, as well as mean HU values between T11–T12 and L1–L2. We used Pearson correlation coefficient to analyze the correlations of HU values with age and lumbar BMD from QCT. Linear regression was used to derive the decline in HU values as a function of participant age. Sensitivity, specificity, and area under the curve (AUC) of the receiver operator characteristic (ROC) curve were calculated and used to evaluate the performance for distinguishing low BMD from normal and osteoporosis from non-osteoporosis. We used the maximum value of Youden index as a criterion to select the optimal HU cutoff threshold from the ROC curve (19). Delong's test was used to assess the difference of the AUC values. A 2-sided $P<0.05$ was considered statistically significant.

Table 1 Participant data and their CT attenuation values in HU for T11 to L2 among normal, osteopenia, and osteoporosis subgroups

Participant	N	Age (years)		T11 HU		T12 HU		L1 HU		L2 HU	
		Mean ± SD	95% CI	Mean ± SD	95% CI	Mean ± SD	95% CI	Mean ± SD	95% CI	Mean ± SD	95% CI
Total	1,112	58.2±8.9	57.7–58.7	172±44	170–175	158±43	156–160	150±41	147–152	145±42	143–148
Female	369	57.9±9.9	56.8–58.8	172±51	166–177	158±51	152–163	149±49	144–154	142±49	137–147
Male	743	58.3±8.4	57.8–58.9	173±40	170–176	158±38	155–161	150±37	147–152	147±38	144–149
Normal	649	55.0±7.4	54.4–55.5	198±34	195–200	183±32	181–186	174±31	172–177	170±32	168–173
Female	206	52.8±7.9	51.8–53.9	205±37	200–210	191±36	186–196	182±34	177–187	175±34	170–179
Male	443	55.9±7.0	55.3–56.6	194±32	191–198	179±29	177–182	170±28	168–173	168±30	165–171
Osteopenia	366	61.1±8.0	60.3–62.0	146±23	143–148	131±21	129–133	124±20	122–126	119±21	117–121
Female	113	61.7±7.0	60.4–63.0	144±24	140–149	130±23	126–135	121±20	118–125	115±22	111–119
Male	253	60.9±8.5	59.8–62.0	146±22	143–149	132±20	129–134	126±20	123–128	121±21	118–123
Osteoporosis	97	68.8±9.3	66.9–70.7	103±27	98–109	90±26	85–95	81±25	76–86	80±31	74–87
Female	50	70.0±8.8	67.7–72.5	97±26	91–104	84±28	77–92	76±26	70–84	72±27	65–79
Male	47	67.2±9.7	64.6–70.2	110±27	102–118	97±23	90–104	85±23	79–92	88±33	79–99

CT, computed tomography; HU, Hounsfield units; SD, standard deviation; CI, confidence interval.

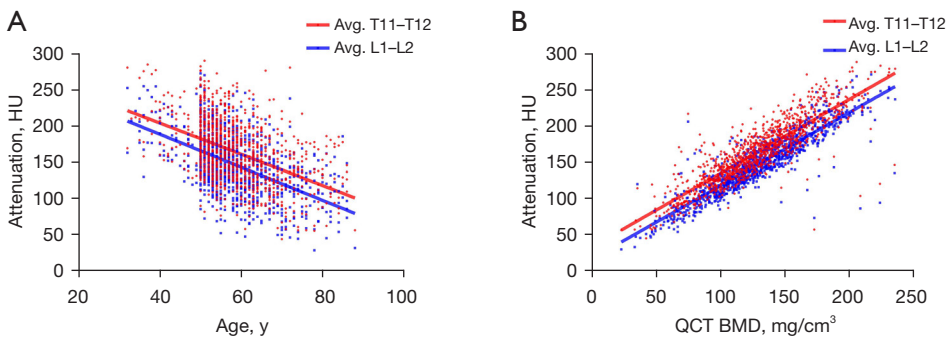

Figure 2 The scatter plot of average CT attenuation values of each vertebral combination with age and lumbar BMD from QCT. HU, Hounsfield units; y, years; Avg., average; QCT, quantitative computed tomography; BMD, bone mineral density; CT, computed tomography.

Results

Participant data

Table 1 shows the demographic information of all participants and their CT attenuation data stratified by the QCT categories of normal, osteopenia, and osteoporosis. Among the 3 groups of bone status, the HU values of T11 to L2 were lowest in the osteoporosis subgroup and highest in the normal subgroup, and the HU values were significantly different (P<0.001). There was no significant difference in age and HU values of T11 to L2 between females and males (P=0.12–0.96). A significant difference was observed in HU values of T11 to L2 (P<0.001), and HU values decreased from T11 to L2 in all participants.

Correlations of HU value with age and QCT BMD

The correlations of HU value with age and QCT BMD are shown in *Figure 2*. There were negative correlations between the mean HU values of 2 vertebral combinations with age of Pearson coefficient of –0.453 (95% CI: –0.498 to –0.405) for T11–T12 and –0.498 (95% CI: –0.541 to –0.453) for L1–L2, respectively (P<0.001). Mean HU values according to age groups are shown in *Figure 3*. The mean HU values showed a linear decrease with age at a rate of 2.1 HU per year for T11–T12 (R^2=0.246) and of 2.3 HU per year for L1–L2

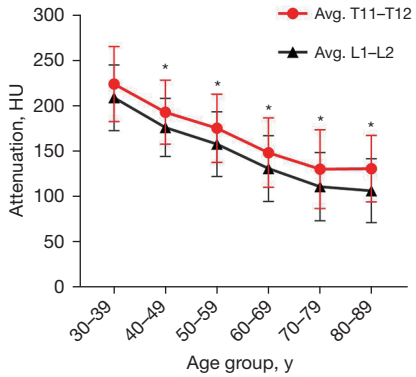

Figure 3 Variations in average CT attenuation values of each vertebral combination according to age groups. Mean trabecular attenuation is higher for T11–T12 than L1–L2 in the age groups (≥40 years) on x-axis (*P<0.05). HU, Hounsfield units; y, years; Avg., average; CT, computed tomography.

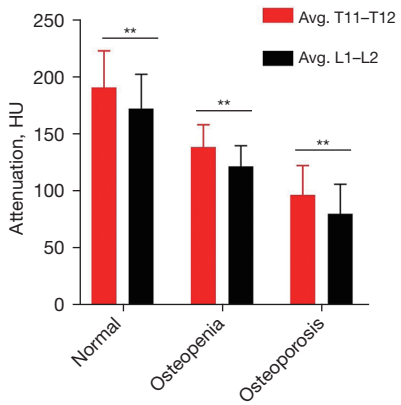

Figure 4 Average CT attenuation values of each vertebral combination, stratified by QCT categories of bone status. The differences in mean HU values between T11–T12 and L1–L2 in each subgroup of bone status were significant (**P<0.001). There were significant differences in mean HU values of T11–T12 and L1–L2 among the three subgroups (P<0.001). HU, Hounsfield units; Avg., average; CT, computed tomography; QCT, quantitative computed tomography.

(R^2=0.286). There were good correlations between the mean HU values of 2 vertebral combinations with lumbar BMD from QCT (T11–T12, r=0.872, 95% CI: 0.857 to 0.886; L1–L2, r=0.899, 95% CI: 0.887 to 0.909; P<0.001). Thus, the mean HU values of T11–T12 also can be used to indirectly reflect the change of lumbar BMD.

HU values of bone status subgroups

Participants were grouped by the QCT-categorized bone status of normal, osteopenia, and osteoporosis. The mean HU values of T11–T12 versus L1–L2 were 190±32 versus 172±30 in the normal subgroup, 138±20 versus 122±18 in the osteopenia subgroup, and 97±26 versus 80±26 in the osteoporosis subgroup (*Figure 4*). There were significant differences in mean HU values of T11–T12 and L1–L2 among 3 bone status subgroups (P<0.001). Thus, the mean HU values of T11–T12 obtained from chest LDCT can be used to classify the bone status of participants. The differences in mean HU values between T11–T12 and L1–L2 in each subgroup of bone status were statistically significant (P<0.001). This implied that establishment of the cutoff thresholds based on mean HU values of T11–T12 for bone status assessment was essential in chest CT imaging.

Cutoff thresholds of CT attenuation values and ROC curves

We derived optimal cutoff thresholds using HU values of T11 to L2 and mean HU values of T11–T12 and L1–L2 to maximize the sensitivity and specificity for low BMD and osteoporosis screening using the Youden index in the ROC curve analysis (*Table 2*). The optimal cutoff thresholds for distinguishing low BMD from normal were average T11–T12 ≤157 HU (AUC =0.941, 95% CI: 0.925–0.954, P<0.001) and L1–L2 ≤138 HU (AUC =0.950, 95% CI: 0.935–0.962, P<0.001). For distinguishing osteoporosis from non-osteoporosis, the optimal cutoff thresholds were average T11–T12 ≤125 HU (AUC =0.960, 95% CI: 0.947–0.971, P<0.001) and L1–L2 ≤107 HU (AUC =0.961, 95% CI: 0.948–0.972, P<0.001). There was no significant difference between the AUC values of T11–T12 and L1–L2 for distinguishing low BMD from normal (P=0.07) and osteoporosis from non-osteoporosis (P=0.92) in *Figure 5*. This suggested that assessment using the mean HU values of T11–T12 and L1–L2 can be used interchangeably for low BMD and osteoporosis screening. Moreover, the cutoff thresholds of T11–T12 and L1–L2 had no significant difference in diagnostic performance for distinguishing low BMD from normal between males and females (P=0.10, P=0.05, respectively), as well as between the participants aged less than 60 years and that aged 60 years or older (P=0.31, P=0.41, respectively, showed in Table S1). Given

Table 2 Performance characteristics of cutoff thresholds of CT attenuation values in HU, for distinguishing low BMD (osteopenia and osteoporosis) from normal, and for distinguishing osteoporosis from non-osteoporosis (normal and osteopenia)

Vertebrae	Distinguishing low BMD from normal				Distinguishing osteoporosis from non-osteoporosis			
	Cutoff HU	Sensitivity, %	Specificity, %	AUC mean (95% CI)	Cutoff HU	Sensitivity, %	Specificity, %	AUC mean (95% CI)
T11	≤161 (0.712[Y])	82.94	88.29	0.924 (0.907–0.939)	≤121 (0.779[Y])	82.47	95.47	0.950 (0.936–0.962)
	≤172	90.06	77.66		≤136	91.75	86.11	
T12	≤146 (0.731[Y])	82.94	90.14	0.936 (0.920–0.950)	≤109 (0.825[Y])	87.63	94.88	0.957 (0.944–0.968)
	≤156	91.79	80.43		≤120	92.78	89.46	
L1	≤141 (0.737[Y])	85.10	88.60	0.941 (0.926–0.954)	≤106 (0.850[Y])	91.75	93.20	0.965 (0.952–0.975)
	≤146	90.06	80.89		≤120	93.81	83.15	
L2	≤135 (0.766[Y])	87.26	89.37	0.938 (0.923–0.952)	≤99 (0.824[Y])	87.63	94.78	0.942 (0.926–0.955)
	≤142	90.28	82.28		≤107	90.72	89.75	
Avg. T11–T12	≤157 (0.740[Y])	87.04	86.90	0.941 (0.925–0.954)	≤125 (0.822[Y])	90.72	91.43	0.960 (0.947– 0.971)
	≤170	94.38	72.57		≤130	92.78	86.50	
Avg. L1–L2	≤138 (0.775[Y])	86.61	90.91	0.950 (0.935–0.962)	≤107 (0.839[Y])	91.75	92.12	0.961 (0.948–0.972)
	≤150	94.82	75.04		≤110	93.81	89.95	

[Y] represented Youden index and corresponding cutoff is optimal cutoff. CT, computed tomography; HU, Hounsfield units; BMD, bone mineral density; AUC, area under the curve; CI, confidence interval; Avg., average CT attenuation values of each vertebral combination.

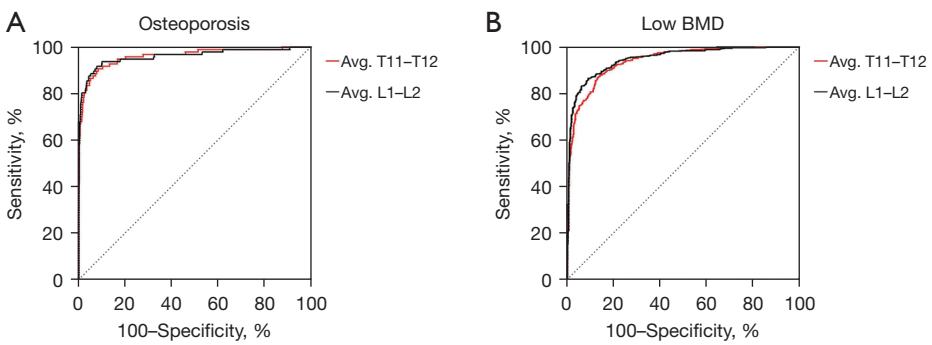

Figure 5 Receiver operating characteristic curves for distinguishing osteoporosis from non-osteoporosis (A) and low BMD from normal (B) using the average CT attenuation values of each vertebral combination, when compared to QCT-defined diagnoses. Avg., average; BMD, bone mineral density; CT, computed tomography; QCT, quantitative computed tomography.

that screening work is focused relatively on sensitivity and convenience, we also reported the cutoff HU values resulting in sensitivity more than 90%, as displayed in *Table 2*.

Discussion

The utilization of chest LDCT scans, ordered for lung cancer screening, may improve the screening rate of patients

with low BMD and osteoporosis at no additional radiation exposure to patients (18). Our study helps to establish the cutoff thresholds of HU values at each T11 to L2 level, and the lower thoracic levels (T11–T12) as well as upper lumbar levels (L1–L2) for opportunistic screening of low BMD and osteoporosis using chest LDCT. We derived optimal cutoff thresholds of average T11–T12 ≤157 HU and L1–L2 ≤138 HU for distinguishing low BMD from normal, and average T11–T12 ≤125 HU and L1–L2 ≤107 HU for distinguishing osteoporosis from non-osteoporosis. Our results showed that assessment of mean attenuation values of T11–T12 and L1–L2 in chest CT images can be used interchangeably for low BMD and osteoporosis screening.

In our study, there was no significant difference in age and HU values of T11 to L2 between women and men (P=0.12–0.96). Thus, HU values of T11 to L2 match quite closely between women and men, although fracture risks may differ because of other factors. Osteoporosis is underappreciated in men and often perceived as a disease that predominately affects postmenopausal women (20). Large population data show that the rate of vertebral fracture is higher in men aged 50–64 years than in women of similar age (21). The opportunistic use of chest LDCT for low BMD and osteoporosis screening may further raise awareness that men can also be at high risk of vertebral fracture. Our results were consistent with a recent study (22) published on the negative correlation between mean HU values and age for the spine. Among a White population, Jang *et al.* (14) found that age-related bone density loss measured by using L1 trabecular attenuation values averaged 2.5 HU per year. With similar results, we found that age-related bone density loss measured by using mean trabecular attenuation values averaged 2.1 HU per year for T11–T12 and 2.3 HU per year for L1–L2 in a Chinese population.

There were significant differences in the distribution of HU values of T11 to L2 among participants with different bone status categories (normal, osteopenia, and osteoporosis, P<0.001) in this study. Therefore, use of these vertebrae from chest LDCT can distinguish different bone status. Our results were consistent with that of the former study (12). Previous studies have revealed a positive correlation between HU values obtained with different CT protocols and BMD form DXA (12,15,22,23). Park *et al.* (12) showed that HU values from each protocol (abdomen/pelvis contrast-enhanced CT, lumbar spine CT, and chest LDCT) were correlated (r=0.676–0.735, P<0.005) with DXA BMD. Chest LDCT had the highest diagnostic performance (AUC =0.701) for diagnosing osteoporosis (12). The association of L1 trabecular attenuation values and T-score appeared to be changed over time and the degree of correlation tended to decrease slightly over time, which was because osteophyte formation and degenerative scoliosis caused errors in DXA results with age (15). L1 and L2 are the current frequently-used vertebrae for QCT diagnosis (16,17). We found that HU measurements of the lower thoracic vertebrae (T11 and T12) and upper lumbar vertebrae (L1 and L2) had positive and significant correlation with lumbar BMD from QCT. Their correlations were close (T11–T12, r=0.872; L1–L2, r=0.899; P<0.001). Thus, the mean HU values of lower thoracic vertebrae in chest LDCT images also can be used to indirectly reflect the change of lumbar BMD.

In this study, there was significant difference in HU values of T11 to L2 (P<0.001), and HU values decreased from T11 to L2 in all participants. Our results coincide with those of a former study (22) which showed that HU values declined from T10 to L1 in each group of bone status. Thus, the use of specific vertebral bodies and cutoff HU values is necessary for assessing bone status. Previous studies sought to establish cutoff HU values for the diagnosis of osteoporosis and low BMD by correlating BMD from DXA. An L1 trabecular attenuation value <100 HU was suggestive of osteoporosis and a high risk of fracture (14). Li *et al.* (24) established optimal cutoff thresholds in terms of mean HU values of L1–L5 for diagnosing (≤136 HU, AUC =0.86) and excluding (≥175 HU, AUC =0.97) osteoporosis on sagittal images from abdominal CT. Compared to DXA, HU measurements on sagittal and transverse images were in agreement to each other (25). A cutoff threshold of L1 ≤135 HU for detecting osteoporosis and a cutoff threshold of L1 ≥160 HU for excluding low BMD provided the sensitivity and specificity in the range from 70.6% to 75.5% (26). Buckens *et al.* (27) determined that the cutoff threshold of L1 ≤99 HU/T12 ≤104 HU had diagnostic performance sensitivity of 62% and specificity of 79% for osteoporosis. Kim *et al.* (28) suggested higher cutoff thresholds for LDCT-measured mean HU values of 4 vertebrae (T4, T7, T10, and L1) for diagnosing osteoporosis in women and men, at 137.9 HU (AUC =0.867) and 136.2 HU (AUC =0.886), respectively. A low BMD cutoff threshold of 167 HU measured on T4 vertebra provided the sensitivity of 80.9% and specificity of 60.5% (29). Using QCT as the reference standard, our optimal cutoff thresholds for distinguishing low BMD from normal were average T11–T12 ≤157 HU (AUC =0.941) and L1–L2 ≤138 HU (AUC =0.950), and those distinguishing osteoporosis from non-

osteoporosis were average T11–T12 ≤125 HU (AUC =0.960) and L1–L2 ≤107 HU (AUC =0.961). The cutoff HU values were slightly different in aforementioned studies. The underlying reason may represent difference in the level of vertebra bodies, the ROI used, and BMD reference (DXA or QCT), or be due to variable ethnicity in the study cohorts (14,30).

DXA measurements may vary depending on the machine used, different detectors, different dual-energy methods, calibration differences, and different reference standards (31). DXA is 2-dimensional assessment and prone to under-detecting patients with osteoporosis, which perpetuates the problem of this condition being both underdiagnosed and undertreated (18). Since the trabecular bone has a high bone turnover rate, it is a bone structure that most accurately reflects bone evaluation, responding sensitively to metabolic stimuli (32). In our study, we adopted the QCT for category reference of bone status as it selectively measures trabecular BMD and is superior to DXA in terms of diagnostic performance (32,33), and because both HU and QCT measurement are performed on CT images. Although a recent study reported by Wáng *et al.* (34) argued that the QCT cutoff value for classifying osteoporosis among older East Asian women will be close to and no more than 50 mg/cm^3 lumbar BMD, we still adopted the generally accepted American College of Radiology QCT diagnostic criteria (17) to define bone status in this study. Given that screening work is focused relatively on sensitivity and convenience, we also reported the cutoff HU values resulting in sensitivity more than 90%. In this study, the cutoff HU values of average T11–T12 ≤170 HU had 94.38% sensitivity and 72.57% specificity for distinguishing low BMD from normal, and average T11–T12 ≤130 HU had 92.78% sensitivity and 86.50% specificity for distinguishing osteoporosis from non-osteoporosis, respectively.

Although vertebral attenuation values can be measured on routine chest CT, such findings are not usually reported clinically. This is mainly because of the lack of established reference standards and the high burden on radiologists resulting from the ever-increasing number of imaging examinations performed. Implementation of artificial intelligence (AI)-based algorithms for CT-based opportunistic abnormal BMD screening is appealing. Although the ability to predict BMD based on attenuation levels using AI has been shown (35), Breit *et al.* (36) reported results in line with a moderate but statistically significant correlation (r=0.34, P=0.01) between the AI-based mean HU values of the thoracic spine (T1–T12) and the lumbar BMD from DXA. The highest diagnostic accuracy to distinguish between participants with normal and low BMD based on the mean HU values of T1–T12 was achieved for 127.7 HU (AUC =0.8) (36). When Sebro *et al.* (37) used the AI-based algorithm to measure attenuation values of multiple bones for predicting osteopenia/osteoporosis, a threshold of 192.1 HU at T4 had highest AUC of 0.757 for predicting osteopenia/osteoporosis using DXA as reference standard. There is no difference between automatic and manual HU measurements with the same ROI (14). Compared to the visual diagnosis made by the reporting radiologists, using the AI-based algorithm with such cutoff thresholds showed a superior diagnostic performance (36). In this study, we automatically extracted the 3D ROI from vertebral body annotation and measured HU values, as well as achieved good performance. We suggested reporting HU values of at least 2 vertebrae in opportunistic screening utilizing AI algorithms, so that any relatively large differences in HU values among vertebral bodies may be brought to the attention of radiologists who review the chest LDCT images and unsuitable measurement conditions.

Our study had a few limitations. Due to the retrospective single-center nature, the generalizability of our results may be somewhat limited. Furthermore, unequal distribution within subgroups of bone status may hinder the use of cutoff HU values that can readily be applied in the general population. Additionally, the influence of different acquisition techniques and scanners need to be investigated in a dedicated manner in future studies. Larger cohorts are needed to establish accurate attenuation thresholds to discriminate osteoporosis and osteopenia from normal. Further work needs to be performed to evaluate how using the HU values from different vertebrae predicts future fracture risk. Despite these limitations, our study still demonstrated that opportunistic screening with lower thoracic vertebrae in chest LDCT scans is feasible and comparable with upper lumbar vertebrae. Since undiagnosed low BMD and osteoporosis are often encountered in daily clinical practice, we hope that this study will further promote opportunistic screening by using trabecular attenuation values of lower thoracic vertebrae in chest LDCT. Our study provides a reference point for physicians to further examine patients for low BMD and osteoporosis.

Conclusions

There was good correlation between CT attenuation

values from chest LDCT and BMD from QCT in this Chinese population. The cutoff HU values of T11 to L2 for low BMD and osteoporosis screening using chest LDCT have been provided. In addition, we have provided cutoff thresholds of average T11–T12 versus L1–L2 to distinguish low BMD (≤157 *vs.* 138 HU) from normal and osteoporosis (≤125 *vs.* 107 HU) from non-osteoporosis. These can serve as a quick reference at chest LDCT to identify patients with abnormal BMD who are at risk for fracture. Opportunistic screening with lower thoracic vertebrae in chest LDCT scans conducted for lung cancer screening is feasible and comparable with upper lumbar vertebrae. Assessment of mean attenuation values of T11–T12 and L1–L2 can be used interchangeably for low BMD and osteoporosis screening using chest LDCT. When the dubiety of low BMD and osteoporosis is raised on chest LDCT, we suggest performing DXA or QCT to verify the diagnosis. We recommend using an automated tool for HU measurement on chest LDCT images to alert patients and physicians to facilitate further early clinical confirmation and management to prevent fractures.

Acknowledgments

Funding: This study received funding from the National Natural Science Foundation of China (Grant No. 82302303), and Medical Science and Technology Project of Zhejiang Province (Grant Nos. 2022PY038, 2023KY493, 2023KY452 and 2024KY625).

Footnote

Reporting Checklist: The authors have completed the STARD reporting checklist. Available at https://qims.amegroups.com/article/view/10.21037/qims-24-59/rc

Conflicts of Interest: All authors have completed the ICMJE uniform disclosure form (available at https://qims.amegroups.com/article/view/10.21037/qims-24-59/coif). H.G.W. reports that he is an employee of Hithink RoyalFlush Information Network Co., Ltd. and Zhejiang Herymed Technology Co., Ltd. He also reports the technical support from Hithink RoyalFlush Information Network Co., Ltd. and Zhejiang Herymed Technology Co., Ltd. The other authors have no conflicts of interest to declare.

Ethical Statement: The authors are accountable for all aspects of the work in ensuring that questions related to the accuracy or integrity of any part of the work are appropriately investigated and resolved. The study was conducted in accordance with the Declaration of Helsinki (as revised in 2013). The study was approved by the Ethics Committee at Zhejiang Provincial People's Hospital (IRB No. 2021QT236) and the requirement for individual consent for this retrospective analysis was waived.

References

1. Kushwaha NS, Singh A, Kumar S, Kumar D, Bharat A. Validation of Quantitative Ultrasonography for Osteoporosis Diagnosis in Postmenopausal Women Compared to Dual-Energy X-Ray Absorptiometry (DEXA). Cureus 2023;15:e38562.
2. Klintström B, Henriksson L, Moreno R, Malusek A, Smedby Ö, Woisetschläger M, Klintström E. Photon-counting detector CT and energy-integrating detector CT for trabecular bone microstructure analysis of cubic specimens from human radius. Eur Radiol Exp 2022;6:31.
3. Aibar-Almazán A, Voltes-Martínez A, Castellote-Caballero Y, Afanador-Restrepo DF, Carcelén-Fraile MDC, López-Ruiz E. Current Status of the Diagnosis and Management of Osteoporosis. Int J Mol Sci 2022;23:9465.
4. Yao Q, Liu M, Yuan K, Xin Y, Qiu X, Zheng X, Li C, Duan S, Qin J. Radiomics nomogram based on dual-energy spectral CT imaging to diagnose low bone mineral density. BMC Musculoskelet Disord 2022;23:424.
5. DXA Testing by the Numbers-Updated: Bone Health & Osteoporosis Foundation. Available online: https://www.bonehealthandosteoporosis.org/wp-content/uploads/Update-State-slides-10-1-19.pdf
6. Wang J, Zhou S, Chen S, He Y, Gao H, Yan L, Hu X, Li P, Shen H, Luo M, You T, Li J, Zhong Z, Zhang K. Prediction of osteoporosis using radiomics analysis derived from single source dual energy CT. BMC Musculoskelet Disord 2023;24:100.

7. Qadan L, Ahmed A. Addressing gaps in osteoporosis screening in kuwait using opportunistic quantitative computer tomography (QCT): a retrospective study. Arch Osteoporos 2023;18:50.
8. Gausden EB, Nwachukwu BU, Schreiber JJ, Lorich DG, Lane JM. Opportunistic Use of CT Imaging for Osteoporosis Screening and Bone Density Assessment: A Qualitative Systematic Review. J Bone Joint Surg Am 2017;99:1580-90.
9. Lee S, Chung CK, Oh SH, Park SB. Correlation between Bone Mineral Density Measured by Dual-Energy X-Ray Absorptiometry and Hounsfield Units Measured by Diagnostic CT in Lumbar Spine. J Korean Neurosurg Soc 2013;54:384-9.
10. Schreiber JJ, Anderson PA, Rosas HG, Buchholz AL, Au AG. Hounsfield units for assessing bone mineral density and strength: a tool for osteoporosis management. J Bone Joint Surg Am 2011;93:1057-63.
11. Lee SJ, Pickhardt PJ. Opportunistic screening for osteoporosis using body CT scans obtained for other indications: the UW experience. Clin Rev Bone Miner Metab 2017;15:128-37.
12. Park J, Kim BR, Lee E, Lee JW. Intra-individual comparison of lumbar spine CT, abdomen-pelvis contrast enhanced CT, and low-dose chest CT for bone density measurement. Acta Radiol 2023;64:1518-25.
13. Alacreu E, Moratal D, Arana E. Opportunistic screening for osteoporosis by routine CT in Southern Europe. Osteoporos Int 2017;28:983-90.
14. Jang S, Graffy PM, Ziemlewicz TJ, Lee SJ, Summers RM, Pickhardt PJ. Opportunistic Osteoporosis Screening at Routine Abdominal and Thoracic CT: Normative L1 Trabecular Attenuation Values in More than 20 000 Adults. Radiology 2019;291:360-7.
15. Lim J, Oh E, Park S, Kim HJ, Yoon YC, Nam B, Lee EJ, Hwang J, Jeong J, Chang YW. Longitudinal Association between L1 Trabecular Attenuation from Chest Computed Tomography (CT) and Bone Mineral Density from Dualenergy X-ray Absorptiometry (DXA). Curr Med Imaging 2023;19:1372-7.
16. Wu Y, Guo Z, Fu X, Wu J, Gao J, Zeng Q, Fu H, Cheng X. The study protocol for the China Health Big Data (China Biobank) project. Quant Imaging Med Surg 2019;9:1095-102.
17. American College of Radiology. ACR–SPR–SSR practice parameter for the performance of musculoskeletal quantitative computed tomography (QCT). Available online: https://www.acr.org/-/media/ACR/Files/Practice-Parameters/QCT pdf. 2018.
18. Naghavi M, De Oliveira I, Mao SS, Jaberzadeh A, Montoya J, Zhang C, Atlas K, Manubolu V, Montes M, Li D, Atlas T, Reeves A, Henschke C, Yankelevitz D, Budoff M. Opportunistic AI-enabled automated bone mineral density measurements in lung cancer screening and coronary calcium scoring CT scans are equivalent. Eur J Radiol Open 2023;10:100492.
19. DeLong ER, DeLong DM, Clarke-Pearson DL. Comparing the areas under two or more correlated receiver operating characteristic curves: a nonparametric approach. Biometrics 1988;44:837-45.
20. Binkley N, Adler R, Bilezikian JP. Osteoporosis diagnosis in men: the T-score controversy revisited. Curr Osteoporos Rep 2014;12:403-9.
21. Ballane G, Cauley JA, Luckey MM, El-Hajj Fuleihan G. Worldwide prevalence and incidence of osteoporotic vertebral fractures. Osteoporos Int 2017;28:1531-42.
22. Yang J, Liao M, Wang Y, Chen L, He L, Ji Y, Xiao Y, Lu Y, Fan W, Nie Z, Wang R, Qi B, Yang F. Opportunistic osteoporosis screening using chest CT with artificial intelligence. Osteoporos Int 2022;33:2547-61.
23. Cohen A, Foldes AJ, Hiller N, Simanovsky N, Szalat A. Opportunistic screening for osteoporosis and osteopenia by routine computed tomography scan: A heterogeneous, multiethnic, middle-eastern population validation study. Eur J Radiol 2021;136:109568.
24. Li YL, Wong KH, Law MW, Fang BX, Lau VW, Vardhanabuti VV, Lee VK, Cheng AK, Ho WY, Lam WW. Opportunistic screening for osteoporosis in abdominal computed tomography for Chinese population. Arch Osteoporos 2018;13:76.
25. Lee SJ, Binkley N, Lubner MG, Bruce RJ, Ziemlewicz TJ, Pickhardt PJ. Opportunistic screening for osteoporosis using the sagittal reconstruction from routine abdominal CT for combined assessment of vertebral fractures and density. Osteoporos Int 2016;27:1131-6.
26. Pickhardt PJ, Pooler BD, Lauder T, del Rio AM, Bruce RJ, Binkley N. Opportunistic screening for osteoporosis using abdominal computed tomography scans obtained for other indications. Ann Intern Med 2013;158:588-95.
27. Buckens CF, Dijkhuis G, de Keizer B, Verhaar HJ, de Jong PA. Opportunistic screening for osteoporosis on routine computed tomography? An external validation study. Eur Radiol 2015;25:2074-9.
28. Kim YW, Kim JH, Yoon SH, Lee JH, Lee CH, Shin CS, Park YS. Vertebral bone attenuation on low-dose chest CT: quantitative volumetric analysis for bone fragility

assessment. Osteoporos Int 2017;28:329-38.
29. Vanier AT, Colantonio D, Saxena SK, Rodkey D, Wagner S. Computed Tomography of the Chest as a Screening Tool for Low Bone Mineral Density. Mil Med 2023;188:665-9.
30. Nam HS, Shin MH, Zmuda JM, Leung PC, Barrett-Connor E, Orwoll ES, Cauley JA; Osteoporotic Fractures in Men (MrOS) Research Group. Race/ethnic differences in bone mineral densities in older men. Osteoporos Int 2010;21:2115-23.
31. Garg MK, Kharb S. Dual energy X-ray absorptiometry: Pitfalls in measurement and interpretation of bone mineral density. Indian J Endocrinol Metab 2013;17:203-10.
32. Lee DH, Kim M. Comparative study of lumbar bone mineral content using DXA and CT Hounsfield unit values in chest CT. BMC Musculoskelet Disord 2023;24:94.
33. Harper KD, Clyburn TA, Incavo SJ, Lambert BS. DEXA overestimates bone mineral density in adults with knee replacements. Sports Med Health Sci 2020;2:211-5.
34. Wáng YXJ, Blake GM, Tang SN, Guermazi A, Griffith JF. Quantitative CT lumbar spine BMD cutpoint value for classifying osteoporosis among older East Asian women should be lower than the value for Caucasians. Skeletal Radiol 2024. [Epub ahead of print]. doi: 10.1007/s00256-024-04632-4.
35. Savage RH, van Assen M, Martin SS, Sahbaee P, Griffith LP, Giovagnoli D, Sperl JI, Hopfgartner C, Kärgel R, Schoepf UJ. Utilizing Artificial Intelligence to Determine Bone Mineral Density Via Chest Computed Tomography. J Thorac Imaging 2020;35 Suppl 1:S35-9.
36. Breit HC, Varga-Szemes A, Schoepf UJ, Emrich T, Aldinger J, Kressig RW, Beerli N, Andreas Buser T, Breil D, Derani I, Bridenbaugh S, Gill C, Fischer AM. CNN-based evaluation of bone density improves diagnostic performance to detect osteopenia and osteoporosis in patients with non-contrast chest CT examinations. Eur J Radiol 2023;161:110728.
37. Sebro R, De la Garza-Ramos C. Machine learning for the prediction of osteopenia/osteoporosis using the CT attenuation of multiple osseous sites from chest CT. Eur J Radiol 2022;155:110474.

Cite this article as: Pan YL, Wu YB, Wang HG, Yu TH, He D, Lu XJ, Zhao FF, Ma HF, Wang YJ, Cai YK. Opportunistic use of chest low-dose computed tomography (LDCT) imaging for low bone mineral density and osteoporosis screening: cutoff thresholds for the attenuation values of the lower thoracic and upper lumbar vertebrae. Quant Imaging Med Surg 2024;14(7):4792-4803. doi: 10.21037/qims-24-59

